Journal of Physics: Conference Series **122** (2008) 012018 doi:10.1088/1742-6596/122/1/012018

Power-recycled Michelson interferometer with a 50/50 grating beam splitter

D Friedrich[1], O Burmeister[1], M Britzger[1], A Bunkowski[1], T Clausnitzer[2], S Fahr[2], E-B Kley [2], A Tünnermann[2], K Danzmann[1], and R Schnabel[1]

[1] Albert-Einstein-Institut Hannover, Max-Planck-Institut für Gravitationspyhsik und Institut für Gravitationsphysik der Leibniz Universität Hannover, Callinstr. 38, 30167 Hannover, Germany

[2] Institut für Angewandte Physik, Friedrich-Schiller-Universität Jena, Max-Wien-Platz 1, 07743 Jena, Germany

E-mail: roman.schnabel@aei.mpg.de

Abstract. We designed and fabricated an all-reflective 50/50 beam splitter based on a dielectric grating. This beam splitter was used to set up a power-recycled Michelson interferometer with a finesse of about $\mathcal{F}_{\mathrm{PR}} \approx 880$. Aspects of the diffractive beam splitter as well as of the interferometer design are discussed.

1. Introduction

All current large-scale laser interferometric gravitational-wave detectors use partly transmissive mirrors as 50/50 beam splitters and cavity couplers. Despite the fact that the absorption of the high-quality optics used can be as small as 0.25 ppm/cm [1] resulting thermal effects can still set a limit to the sensitivity of these detectors [2]. In all-reflective interferometer topologies [3, 4, 5, 6] partly transmissive optics are replaced by reflection gratings. In addition to reducing all absorption related thermal effects inside the optics, all-reflective interferometers are capable of using opaque substrate materials and may thus benefit from their thermal and mechanical properties [7]. Since resonator techniques such as power-recycling (PR) [8] are used to increase the circulating light power up to the kilowatt range low loss optics are required. For increasing the sensitivity of high precision laser interferometers we explore the application of optimized dielectric reflection gratings.

In this paper we give an overview of the design and experimental realization of a Michelson interferometer (Mi-ifo) with power-recycling, where the central 50/50 beam splitter was replaced by a custom-built dielectric reflection grating [9]. Although the diffraction at the beam splitter causes the beam profiles to be different in the respective interferometer arms, we achieved a high interference contrast due to a careful design of the experiment. With this setup we determined the overall optical loss of the grating [10].

2. Diffractive beam splitter: design and realization

Dielectric reflection gratings are composed of a substrate, a highly reflective multilayer-stack and a periodic grating profile (see Fig.1(a)). For a grating period d and angle of incidence ϕ_{in}

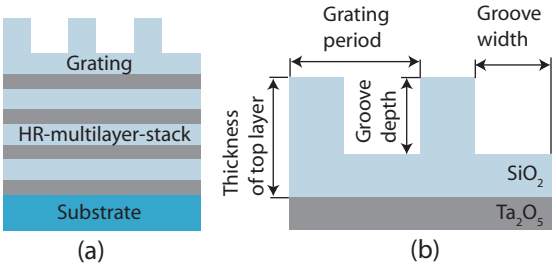

Figure 1. (a) Schematic of a reflection grating based on dielectric materials. (b) Parameters of a binary grating profile that constitute the diffraction properties.

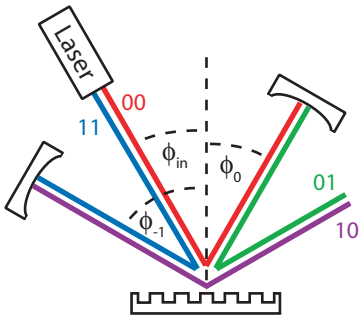

Figure 2. Topology of an all-reflective Michelson interferometer. The diffraction angles (ϕ_0, ϕ_{-1}) are given by the grating equation (1).

the angle of the m-th diffraction order ϕ_m is given by the grating equation

$$\sin(\phi_\mathrm{m}) = \sin(\phi_\mathrm{in}) + \frac{m\lambda}{d}, \tag{1}$$

where λ denotes the wavelength of the laser light. Diffractive devices with two diffraction orders (0th, -1st) are an alternative to transmissive beam splitters. We designed and fabricated an all-reflective 50/50 grating beam splitter for s-polarized light with a wavelength of $\lambda = 1064\,\mathrm{nm}$. For this purpose we explored binary grating structures with a rectangular profile, because they can be routinely produced using microstructure technologies, namely e-beam lithography and ion-beam etching. While the number and directions of diffraction orders only depend on the wavelength and grating period, the diffraction efficiencies for a particular polarization of light depend on all parameters of the grating profile. We used Rigorous Coupled Wave Analysis (RCWA) [11] to calculate the diffraction efficiencies.

For a convenient application of a reflection grating as the central beam splitter in an all-reflective Mi-ifo (see Fig.2) the following demands have to be met: the existence of only two diffraction orders and proper separation of the beams. In order to allow for a classical Mi-ifo design with perpendicular arms it is preferable that the angle between the 0th and -1st diffraction order is 90 °. For a fixed polarization and wavelength the remaining parameters, namely groove depth, grating period, groove width, thickness of the top layer, and index of refraction of used materials (see Fig.1(b)), can be optimized to obtain a 50/50 splitting ratio. An important design concern is to find a design that is as tolerant as possible to variations of the groove parameters during the fabrication process. For this purpose we did various parameter scans leading to sets with sufficient tolerances. Starting point was a high-reflective multilayer-stack consisting of 44 alternating layers of fused silica (SiO_2) and tantalum pentoxide (Ta_2O_5). A detailed analysis [9] led to a top layer thickness of 335 nm, groove depth of 300 nm, groove width of 425 nm, grating period of 790 nm, and angle of incidence of 27 °. This design simultaneously allowed for a 50/50 splitting ratio and a rectangular interferometer configuration. The measured diffraction efficiencies for 0th and -1st order of the fabricated grating were in good agreement with the calculated design values as shown in Fig.3.

3. Interferometer design

An all-reflective Mi-ifo can be operated in much the same way as a conventional Mi-ifo with a transmissive beam splitter. In Fig.2 the different paths at which light enters an all-reflective Mi-ifo are colored. The *antisymmetric* port consists of the light fields that are twice reflected (00)

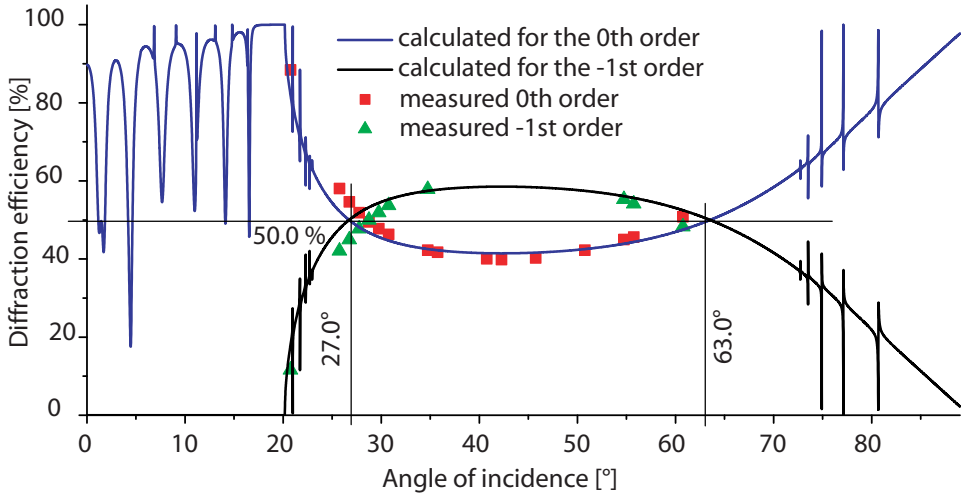

Figure 3. Calculated and measured diffraction efficiencies of the 0th and -1st order.

or diffracted (11). The signal port contains the beams having a *symmetrical* path (01,10). If the microscopic armlengths are adjusted to provide a dark signal port, all laser power is reflected back towards the laser and can be recycled by means of an additional mirror that is placed between the laser and the Mi-ifo, thus forming a Fabry-Perot-Resonator. As seen from the laser a Mi-ifo acts as a compound mirror with variable reflectivity depending on the operation point, the interference contrast at the beam splitter, and additional losses.

For an all-reflective Mi-ifo the diffracted beams in 0th and -1st order have different deflection angles resulting in different beam shapes as is illustrated in Fig.4. An incident beam of circular

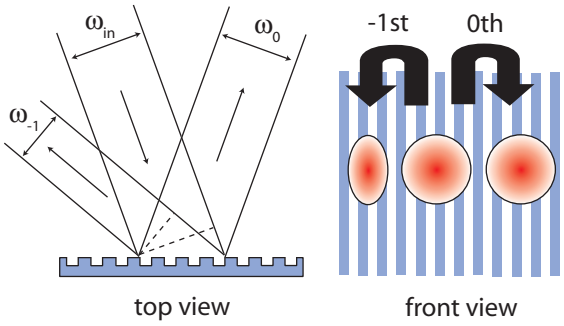

Figure 4. An all-reflective beam splitter always causes the beam profiles of the diffracted beams to be different with respect to each other. This is due to different deflection angles in the diffraction plane for the 0th and -1st diffraction order.

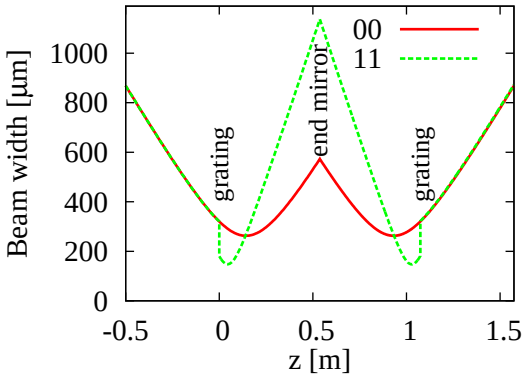

Figure 5. Beam width of the fundamental gaussian mode in the diffraction plane versus propagation z through the experimentally realized interferometer configuration. 00 and 11 denote the beams that are twice reflected and diffracted, respectively (see Fig.2).

shape remains circular in 0th order but is elliptical in -1st order with a changed waist size and position in the diffraction plane [12]. Hence, the beam variation along the propagation in a

Mi-ifo differs for the two arms and it is not sufficient to use an interferometer configuration with equal end mirrors and equal armlengths in order to achieve a good interference contrast.

Using the ABCD-matrix formalism for Gaussian beams we calculated interferometer configurations and according geometries of the incident beam. This was done by taking into account all components of the Mi-ifo. As a result, for the typical case of concave end mirrors the radius of curvature R_c is restricted by

$$L\frac{\cos^2(\phi_{-1})-\cos^2(\phi_0)}{\cos^2(\phi_0)} < R_c < L, \tag{2}$$

where L is the armlength and $\phi_0 < \phi_{-1}$. Within this parameter range the size and position of the waist of the incident beam is fixed by the particular choice of R_c.

The beam width variation in the diffraction plane for a configuration realized in a table top experiment (see below) is shown in Fig.5 for the beams twice reflected (00) and twice diffracted (11). The beam variations perpendicular to the diffraction plane are equal to that of the 00 path. Hence, after propagation through the interferometer the partial beams overlap perfectly. Furthermore the shape of the beam reflected from the interferometer matches the shape of the incident beam. Hence, the interference contrast can be preserved even if an additional power-recycling mirror is installed.

4. Experimental results

The experimental setup of the power-recycled Michelson interferometer with diffractive beam splitter is sketched in Fig.6. The light source was a Nd:YAG laser at 1064 nm, which was spatially

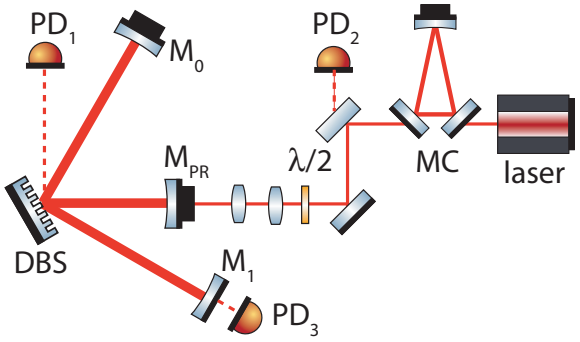

Figure 6. Experimental setup of the power-recycled Michelson interferometer with diffractive beam splitter (DBS), HR-end mirrors (M_0, M_1) and power-recycling mirror (M_{PR}). The laser light was spatially filtered by a triangular modecleaner cavity (MC) and detected with various photodiodes (PD). M_0 and M_{PR} were attached to piezoelectric transducers for controlling the microscopic armlength difference and length of the power-recycling cavity, respectively.

filtered by a triangular ring resonator. For the given grating and angle of incidence of $\phi_{in} \approx 29\,^\circ$ the diffraction angles into the 0th and -1st order were $\phi_0 \approx 29\,^\circ$ and $\phi_{-1} \approx 60\,^\circ$, respectively. The splitting ratio for s-polarized light was found to be $(47.8/52.2 \pm 0.1)\,\%$. Using high-reflectivity end mirrors (M_0, M_1) with radius of curvature $R_c = 0.5\,\mathrm{m}$ we set up a Michelson interferometer with an armlength of $L = 0.537\,\mathrm{m}$, resulting in the beam width variation shown in Fig.5. The interference contrast was determined to be $C = (I_{max} - I_{min})/(I_{max} + I_{min}) = 0.9989 \pm 0.0001$ where I_{max} and I_{min} denote the maximal and minimal power in the signal port, respectively. As the wavefront of the mode reflected by the interferometer has to match the curvature of the power-recycling mirror (M_{PR}) of $R_{pr} = 0.6\,\mathrm{m}$, its position was predefined in order to preserve the interference contrast achieved. To find the optimal position of M_{PR} we measured the power in the signal port (PD1) and in the interferometer (PD3) according to Fig.6, while the Mi-ifo and power-recycling cavity were stabilized to dark port condition and resonance, respectively. The ratio of measured powers was minimal at $l_{PR} = 0.378\,\mathrm{m}$ (see Fig.7), thus giving the lowest power loss in the signal port. The peak at $l_{PR} \approx 0.405\,\mathrm{m}$ was caused by a higher order mode

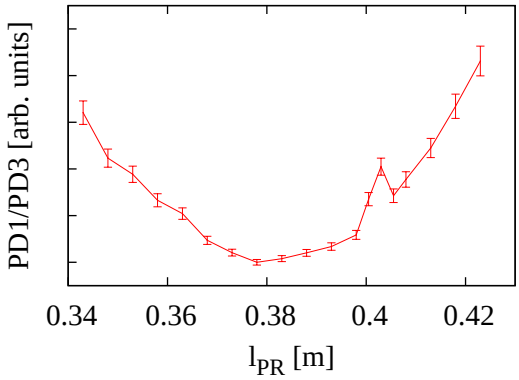

Figure 7. The ratio of power in the dark port and inside the interferometer (PD1/PD3) (see Fig.6 for photodiode positions) was used to identify the optimal power-recycling mirror distance to the beam splitter $l_{\mathrm{PR}} = 0.378\,\mathrm{m}$.

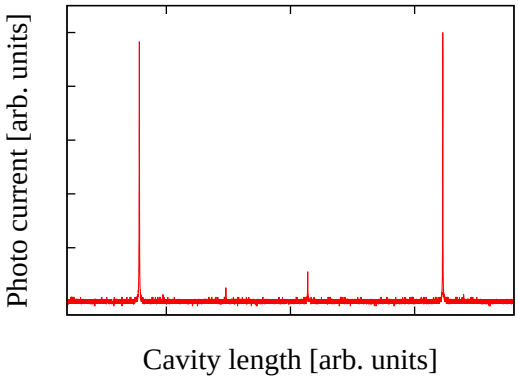

Figure 8. Free spectral range of the power-recycling cavity detected in transmission behind one end mirror of the Mi-ifo. The finesse was determined to be $\mathcal{F}_{\mathrm{PR}} \approx 880$, while the intra cavity loss was about 0.46 %.

that was resonant for this particular cavity length. Fig.8 shows the free spectral range of the power-recycling cavity of finesse $\mathcal{F}_{\mathrm{PR}} = 883 \pm 28$, which was used to determine optical loss inside the cavity [6]. Linear reference cavities built with the mirror combinations (M_0, M_{PR}) and (M_1, M_{PR}) showed an averaged finesse of $\mathcal{F}_{\mathrm{ref}} = 2543 \pm 81$. The decreased finesse of the power-recycling cavity compared to the obtained reference value is caused by an overall additional loss of $(0.463 \pm 0.024)\,\%$ that is due to the remaining loss in the signal port of (781 ± 137) ppm and twice the optical grating loss of $(0.193 \pm 0.019)\%$, which is the sum of transmission, unwanted higher orders due to fabrication errors and scattering. A more detailed description of this characterization and the experimental setup used is given in [10].

5. Conclusion

We presented the experimental realization of a power-recycled Michelson-interferometer with a custom-built dielectric reflection grating as the central beam splitter. A high interference contrast of 0.9989 was achieved due to an interferometer configuration that takes the beam deformation at the grating into account. Further we implemented the power-recycling technique resulting in a finesse of about $\mathcal{F}_{\mathrm{PR}} \approx 880$.

Acknowledgments

This work was supported by the Deutsche Forschungsgemeinschaft (DFG) within the Sonderforschungsbereich TR7.

References

[1] Hild S, Lück H, Winkler W, Strain K, Grote H, Smith J, Malec M, Hewitson M, Willke B, Hough J, and Danzmann K 2006 Appl. Opt. **45** 7269
[2] Winkler W, Danzmann K, Rüdiger A, Schilling R 1991 Phys. Ref. A **44** 7022
[3] Drever R W P 1995 Proceedings of the Seventh Marcel Grossman Meeting on General Relativity, M. Keiser and R. T. Jantzen, eds. (World Scientific, 1995)
[4] Sun K-X and Byer R L 1997 Opt. Lett. **23** 567
[5] Bunkowski A, Burmeister O, Beyersdorf P, Danzmann K, Schnabel R, Clausnitzer T, Kley E-B, and Tünnermann A 2004 Opt. Lett. **29** 2342
[6] Bunkowski A, Burmeister O, Clausnitzer T, Kley E-B, Tünnermann A, Danzmann K, Schnabel R 2006 Appl. Opt. **45** 5795

[7] Rowan S, Byer R L, Fejer M M, Route R, Cagnoli G, Crooks D R M, Hough J, Sneddon P H, Winkler W 2003 Proceedings of SPIE **4856** 292
[8] Schnier D, Mizuno J, Heinzel G, Lück H, Rüdiger A, Schilling R, Schrempel M, Winkler W, Danzmann K 1997 Phys. Lett. A **225** 210
[9] Fahr S, Clausnitzer T, Kley E-B, Tünnermann A 2007 Appl. Opt. **46**, 6092
[10] Friedrich D, Burmeister O, Bunkowski A, Clausnitzer T, Fahr S, Kley E-B, Tünnermann A, Danzmann K, Schnabel R 2007 (Opt. Lett.) **33** 101
[11] Moharam M G, Gaylord T K 1982 J. Opt. Soc. Am. **72**, 1385
[12] Siegman A E 1985 J. Opt. Soc. Am. A **2** 1793